P−B Adducts of 3,4-Dimethyl-1-phosphaferrocene with Bromoboranes

Matthias Scheibitz,[a] Jan W. Bats,[b][‡] Michael Bolte,[b][‡] and Matthias Wagner*[a]

Dedicated to Prof. Dr. Herbert Wagner on the occasion of his retirement

Keywords: Boranes / Donor-acceptor systems / Metallocenes / P ligands / X-ray diffraction

The crystalline adducts FcP–BBr_3 (**2**) and FcP–BBr_2Fc (**3**), which are very rare examples of *P*-bonded complexes between phosphaferrocene and a main-group metal atom, were obtained by the reaction of 3,4-dimethyl-1-phosphaferrocene (FcP) with BBr_3 and $FcBBr_2$ (Fc: ferrocenyl). According to X-ray crystallography, the Fe–P bond length in **2** is 0.085 Å shorter than in the parent phosphaferrocene. All structural changes resulting from P–B acid–base pairing follow the same qualitative trend, but are significantly larger than those occurring from the formation of transition metal complexes of phosphaferrocene. In contrast to **2**, NMR spectroscopy reveals **3** to be almost completely dissociated in $CDCl_3$ solution at room temperature.

(© Wiley-VCH Verlag GmbH & Co. KGaA, 69451 Weinheim, Germany, 2003)

Introduction

Oligonuclear transition metal complexes are receiving great attention because of their numerous applications both in homogeneous catalysis[1] and in materials science.[2] The sandwich complex ferrocene has proven to be a particularly important building block in this context. 1,2-Disubstituted ferrocene derivatives give access to chelate ligands possessing planar chirality that have been employed successfully in asymmetric catalysis.[3−5] In the field of materials science, Manners et al. took advantage of the ring-opening polymerisation of strained *ansa*-ferrocenes for the generation of poly(ferrocenylene)s that exhibit interesting optical and electronical properties.[6] Phosphaferrocenes **A**[7] and 1,1′-diphosphaferrocenes **B**[8] (Figure 1), which became available from the work of Mathey et al., were soon recognized to form stable κ-*P* complexes with various transition metals.[9] Ganter et al. developed appropriately substituted derivatives of **A** as a new class of chiral chelate ligands,[10,11] while **B** was used as bridging unit in the formation of heterotrimetallic aggregates.[12]

Our group recently reported a convenient approach to ferrocene-containing macromolecules that benefits from the facile formation of Lewis acid−base adducts. For example, the reaction of the diborylated ferrocene 1,1′-fc(BMe_2)$_2$ [fc = (C_5H_4)$_2$Fe] with selected difunctional Lewis bases (e.g., pyrazine) gives access to polymeric materials in high yield and under very mild conditions (e.g., **C**, Figure 1).[13−15] We decided to investigate whether the or-

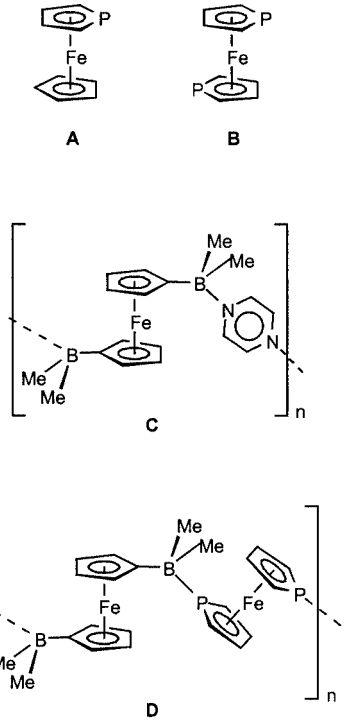

Figure 1. Phosphaferrocene **A**, 1,1′-diphosphaferrocene **B** (only the parent molecules are shown as representatives of the whole class of derivatives), a B−N-bonded charge-transfer coordination polymer **C**, and the final target molecule **D**

[a] Institut für Anorganische Chemie, J. W. Goethe-Universität Frankfurt,
Marie-Curie-Strasse 11, 60439 Frankfurt (Main), Germany
Fax: (internat.) + 49-69/79829260
E-mail: Matthias.Wagner@chemie.uni-frankfurt.de
[b] Institut für Organische Chemie, J. W. Goethe-Universität Frankfurt,
Marie-Curie-Strasse 11, 60439 Frankfurt (Main), Germany
[‡] X-ray crystallography

ganic linker in **C** can be replaced by the redox-active organometallic template ligand **B** to generate target molecules like **D** (Figure 1).

A particular challenge is offered by the fact that despite the plethora of well-characterized complexes of phosphaferrocene and transition metals, no adducts of **A** and only one adduct of **B**[16] with main-group Lewis acids has been isolated so far. In contrast to the related azaferrocene, which is readily quaternized by methyl iodide,[17] diphosphaferrocene **B** was found to react only at elevated temperature, even in neat benzyl bromide. The reaction leads to the decomposition of the phosphaferrocene moiety with liberation of *P*,*P*-dibenzylphospholium bromide.[18] Acetylations, formylations and carboxylations of phosphaferrocenes occur selectively at the α-carbon atoms of the coordinated phospholyl ring.[8,18,19] Moreover, treatment of **A** or **B** with trifluoromethanesulfonic acid leads to protonation on the iron atom, rather than on the phosphorus atom.[20] In summary, the P atom of phosphaferrocenes possesses an energetically low-lying lone pair of electrons and consequently acts as a rather poor σ donor. The LUMO, on the other hand, has pronounced p_z character on the phosphorus atom and is well suited to accept π-electron density.[9,11] The stability of phosphaferrocene-κ-*P*−ML_n complexes is, therefore, expected to grow with an increasing degree of back bonding from electron-rich ML_n fragments. Thus, the fact that main-group elements are not able to have $d_\pi-p_\pi$ interactions with **A** or **B** might explain why corresponding κ-*P* η^1-adducts are virtually unknown up to now. One report on the reaction of phosphaferrocene with $BF_3{\cdot}OEt_2$ has been published that provides evidence for the existence of a phosphorus-bonded adduct in solution (^{31}P NMR spectroscopic control).[20] Moreover, the hypothetical P−B complex $\mathbf{A}{\cdot}BH_3$ has been studied theoretically using DFT methods.[21] Mathey et al. recently reported the reaction of octa-*n*-propyldiphosphaferrocene with $GaCl_3$, which leads to the formation of a tetrahedral gallium(III) complex featuring a chelating diphosphaferrocene ligand.[16] Here, we describe the synthesis, isolation and structural characterization of two P−B adducts of 3,4-dimethyl-1-phosphaferrocene (**1**, Scheme 1).

Results and Discussion

Synthesis and Spectroscopic Characterization

The phosphaferrocene derivative **1** (Scheme 1) was chosen for our investigation because it is accessible in high yield by an established procedure.[7,22] When **1** is treated with the strong Lewis acid BBr_3 in $CDCl_3$ (stoichiometric ratio: 1:1), no obvious reaction takes place since the resulting clear mixture still possesses the orange colour of the initial phosphaferrocene solution. NMR spectroscopy at ambient temperature, however, reveals significant shifts of some characteristic resonances. The phosphorus nucleus in **2** [$\delta(^{31}P) = -13.2$ ppm, $h_{1/2} = 30.1$ Hz] is deshielded by 69.3 ppm compared to that of the free ligand **1** [$\delta(^{31}P) = -82.5$ ppm, $h_{1/2} = 6.5$ Hz]. A strong downfield shift of the

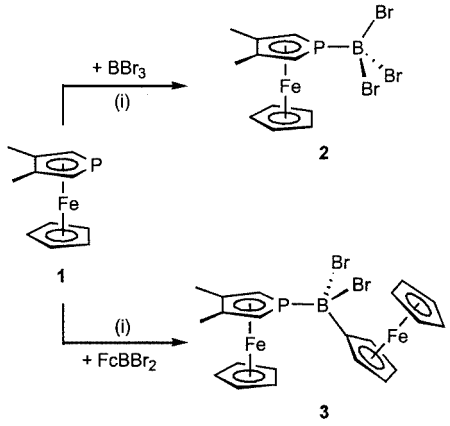

Scheme 1. Synthesis of the P−B-bonded phosphaferrocene adducts **2** and **3**; (i) ambient temperature, C_6H_6

^{31}P NMR signal is also generally observed upon complexation of phosphaferrocenes with transition metal ions.[9] No signal is detectable in the ^{11}B NMR spectrum, which is most likely due to severe line broadening resulting from a dynamic adduct equilibrium. In the ^1H NMR spectrum of **2**, and with respect to parent 3,4-dimethyl-1-phosphaferrocene [**1**: $\delta(^1H) = 3.74$ ($^2J_{P,H} = 36.3$ Hz, phospholyl α-C*H*), 4.15 (C_5H_5) ppm], the resonances of the phospholyl α-protons [**2**: $\delta(^1H) = 4.18$ ($^2J_{P,H} = 29.1$ Hz) ppm] and the cyclopentadienyl ring [**2**: $\delta(^1H) = 4.55$ ppm] are shifted to lower field by 0.44 ppm and 0.40 ppm, respectively. Moreover, the $^2J_{P,H}$ coupling constant decreases by 7.2 Hz. Both the ^{31}P and ^{11}B NMR spectra were recorded also at −50 °C ($CDCl_3$). Under these conditions, the ^{31}P NMR resonance appears at $\delta = -12.9$ ppm as a well-resolved quadruplet with intensity ratios of 1:1:1:1 and a coupling constant of $^1J_{P,B} = 138.5$ Hz ($^1J_{P,B}$ values have been reported within a range of 10−180 Hz[23]). The ^{11}B NMR signal possesses a chemical shift value of $\delta = -20.9$ ppm (d, $^1J_{P,B} = 138.5$ Hz). Consequently, at −50 °C the solution contains mainly the adduct **2**, rather than free **1** and BBr_3.

The ^{11}B and ^1H NMR spectra of an equimolar mixture of **1** with $FcBBr_2$ in $CDCl_3$ at ambient temperature show only negligible differences to the NMR spectra of the individual components. In the ^{13}C NMR spectrum of **1**/$FcBBr_2$, the doublet of the phospholyl α-carbon atoms is broad, while the other signals remain unchanged. The chemical shift of the ^{31}P NMR resonance is the same in **1**/$FcBBr_2$ as in the case of **1**, but the width at half height increases from $h_{1/2} = 6.5$ Hz (**1**) to $h_{1/2} = 165.6$ Hz (**1**/$FcBBr_2$). Thus, NMR spectroscopy reveals the Lewis acid−base pair **1**/$FcBBr_2$ to be almost completely dissociated at room temperature in $CDCl_3$ solution. Slow evaporation of an equimolar mixture of **1** and $FcBBr_2$ in benzene, however, yielded X-ray-quality crystals of the desired P−B-bonded dinuclear species **3**.

X-ray Crystal Structure Determination

The phosphaferrocene−borane adducts **2** and **3** crystallize from benzene in the space groups *Pna*2_1

 © 2003 Wiley-VCH Verlag GmbH & Co. KGaA, Weinheim

(orthorhombic) and $P2_1/c$ (monoclinic), respectively (Table 1). A comparison of the molecular geometries of **1**, **2** (Figure 2) and **3** (Figure 3) reveals remarkable structural changes as a result of P−B bond formation (Table 2). The Fe(1)−P(1) bond length in the BBr_3 adduct **2** possesses a value of 2.199(2) Å, which is 0.085 Å shorter than the iron−phosphorus bond in the parent 3,4-dimethyl-1-phosphaferrocene (**1**) [2.284(1) Å].[24] $FcBBr_2$ is known to be a weaker Lewis acid than BBr_3 because the ferrocenyl substituent acts as an electron donor towards the formally empty p orbital of the boron atom.[25] Consequently, the length of the Fe(1)−P(1) bond in **3** [2.216(1) Å] is intermediate between the values determined for **1** and **2**. These findings are consistent with the general trend observed for transition metal complexes of phosphaferrocenes. A search of the Cambridge Structural Database (CSD, Version 5.24, November 2002)[26] reveals the average Fe−P bond length in monophosphaferrocene derivatives to be 2.285(13) Å (10 structures). This value is reduced to 2.238(16) Å in the corresponding phosphorus-bonded transition metal complexes (22 structures). Interestingly, the effect of Fe−P bond contraction is larger in the borane adducts **2** and **3** than in the corresponding transition metal complexes. P−B acid−base pairing also has a pronounced influence on the C(2)−P(1)−C(5) angle, which is stretched from 88.9(2)° in **1** to 94.7(4)° in **2**, and to 92.7(2)° in **3**. Again, these findings are in good qualitative agreement with the structural features obtained for phosphaferrocene−transition metal aggregates [C−P−C angle in free phosphaferrocene (mean value of 10 derivatives): 89(1)°; C−P−C angle in phosphaferrocene−transition metal complexes (mean value of 22 structures): 92(1)°]. Thus, in all phosphaferrocene derivatives investigated so far (including **2** and **3**), a long Fe−P bond appears to be associated with a small C−P−C angle. It has to be noted that the degree of phospholyl ring puckering is largely unaffected by P−B bond formation. In the case of **1**, the P atom is located at a position 0.048(1) Å above the C(2)C(3)C(4)C(5) plane, while in **2** this displacement is only slightly reduced to a value of 0.043(1) Å. Thus, the phosphorus atom is not just pulled toward the iron centre upon coordination of BBr_3, which would result in a flattening of the phospholyl ligand, but rather it moves toward the C(3)−C(4) bond along a line almost parallel to the C(2)C(3)C(4)C(5) plane {**1**: *d*[P(1)···MP] = 2.589 Å; **2**: *d*[P(1)···MP] = 2.504 Å; MP: midpoint of the C(3)−C(4) bond}. As a result, the P−Fe bond, as well as the P−C bonds, become shorter [cf. **1**: P(1)−C(2) = P(1)−C(5) = 1.774(3) Å; **2**: P(1)−C(2) = P(1)−C(5) = 1.745(8) Å], the C−P−C angle increases, and the adjacent P−C−C angles decrease [cf. **1**: P(1)−C(2)−C(3) = 113.9(2)°, P(1)−C(5)−C(4) = 114.0(2)°; **2**: P(1)−C(2)−C(3) = 109.0(5)°, P(1)−C(5)−C(4) = 110.0(5)°]. The differences observed between the geometrical parameters of **1** and **3** are rather similar to those described above for **1** and **2** and, thus, do not merit further discussion. The P(1)−B(1) bond in **2** [1.972(9) Å] is 0.051 Å shorter than in **3** [2.023(4) Å]. The bond angles around the boron atoms cover a range between P(1)−B(1)−Br(3) = 104.9(4)° and Br(1)−B(1)−Br(3) = 112.2(4)° in the case of **2**, and P(1)−B(1)−Br(1) = 102.9(2)° and C(21)−B(1)−Br(1) = 114.2(2)° in the case of **3**. The relevant Br−B−Br angles of 110.9(4)°, 111.9(4)°, and 112.2(4)° in **2** are slightly larger than the value expected for an sp^3-hybridized boron atom with ideal tetrahedral geometry (109.5°). In **3**, the boron centre is somewhat less pyramidalized, which, together with the longer P(1)−B(1) bond, again indicates a weaker acid−base interaction as is the case in **2**. This interpretation is in agreement with the conclusions drawn from our NMR spectroscopic studies (see above). The BBr_3 adduct **2** features a torsion angle C(2)−P(1)−B(1)−Br(2) of 85.4(5)°. A similar conformation is observed in **3** for the BBr_2P fragment with respect to the ferrocenyl substituent [C(22)−C(21)−B(1)−P(1) = −87.9(3)°], whereas, com-

Table 1. Selected crystallographic data for **2** and **3**

Compound	**2**	**3**
Formula	$C_{11}H_{13}BBr_3FeP$	$C_{21}H_{22}BBr_2Fe_2P$
M	482.57	587.69
Crystal system	orthorhombic	monoclinic
Space group	$Pna2_1$	$P2_1/c$
a [Å]	14.1040(10)	10.561(3)
b [Å]	15.5060(10)	22.221(5)
c [Å]	6.9450(9)	8.8365(17)
β [°]	90	97.366(14)
V [$Å^3$]	1518.8(2)	2056.5(8)
Z	4	4
D_c [g cm^{-3}]	2.110	1.898
T [K]	173(2)	144(2)
μ(Mo-K_α) [mm^{-1}]	8.965	5.378
$2\theta_{max.}$ [°]	56.56	65.42
Measured reflections	25504	36221
Unique reflections (R_{int})	3772 (0.083)	7009 (0.072)
Observed reflections [$I > 2\sigma(I)$]	3174	4777
Parameters refined	157	246
*R*1 [$I > 2\sigma(I)$]	0.051	0.051
*wR*2 [$I > 2\sigma(I)$]	0.121	0.080
GOOF on F^2	1.031	1.074
Largest diff. peak/hole [e·$Å^{-3}$]	0.74/−0.83	1.13/−0.65

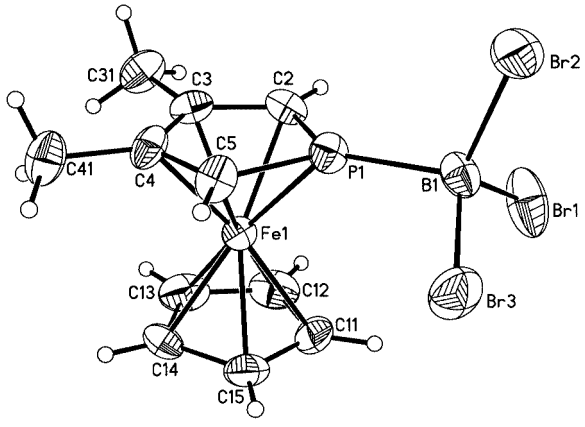

Figure 2. Molecular structure and numbering scheme of compound **2**; thermal ellipsoids shown at the 50% probability level

 © 2003 Wiley-VCH Verlag GmbH & Co. KGaA, Weinheim

pared to compound **2**, the phosphaferrocene moiety is rotated by almost 180° about the P(1)−B(1) bond [C(2)−P(1)−B(1)−C(21) = −90.8(3)°]. This conformation results in a short intramolecular C−H···π interaction between the C(11)−H(11) bond and the cyclopentadienyl ring C(21)C(22)C(23)C(24)C(25) [H(11)···Cg = 2.68 Å, C(11)−H(11)···Cg = 152°; Cg: centroid of the cyclopentadienyl ligand]. Both the ferrocene and phosphaferrocene groups have approximately eclipsed conformations. In **3**, the angle between the planes of the five-membered rings is 1.7° for the ferrocenyl group and 4.2° for the phosphaferrocene moiety.

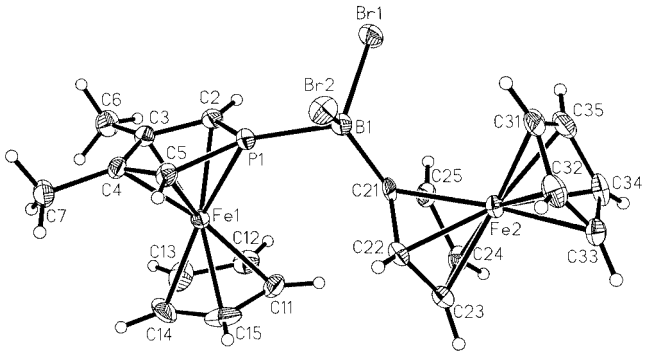

Figure 3. Molecular structure and numbering scheme of compound **3**; thermal ellipsoids shown at the 50% probability level

Table 2. Selected bond lengths [Å], angles [°] and torsion angles [°] of **1**,[24] **2** and **3**; Note: The atom labels of compound **1** have been adapted to the numbering scheme of **2** and **3**

Compound	**1** (T = 74 K)	**2** (T = 173 K)	3 (T = 144 K)
Fe(1)−P(1)	2.284(1)	2.199(2)	2.216(1)
Fe(1)−C(2)	2.072(2)	2.075(7)	2.076(3)
Fe(1)−C(3)	2.057(2)	2.070(7)	2.066(3)
Fe(1)−C(4)	2.054(2)	2.073(7)	2.062(3)
Fe(1)−C(5)	2.060(2)	2.095(7)	2.075(3)
P(1)−C(2)	1.774(3)	1.745(8)	1.744(3)
P(1)−C(5)	1.774(3)	1.745(8)	1.741(3)
C(2)−C(3)	1.424(4)	1.441(11)	1.420(4)
C(3)−C(4)	1.436(3)	1.438(10)	1.427(4)
C(4)−C(5)	1.422(4)	1.431(10)	1.419(4)
P(1)−B(1)	−	1.972(9)	2.023(4)
C(2)−P(1)−C(5)	88.9(2)	94.7(4)	92.7(2)
P(1)−C(2)−C(3)	113.9(2)	109.0(5)	110.9(2)
P(1)−C(5)−C(4)	114.0(2)	110.0(5)	111.1(2)
C(2)−C(3)−C(4)	111.6(2)	113.7(6)	112.7(3)
C(5)−C(4)−C(3)	111.6(2)	112.6(6)	112.7(3)
C(2)−P(1)−B(1)−Br(2)	−	85.4(5)	−
C(2)−P(1)−B(1)−C(21)	−	−	−90.8(3)

Conclusion

In contrast to the rich chemistry that has been developed for complexes between phosphaferrocene and transition metals, examples of *P*-bonded adducts between phosphaferrocene and main-group Lewis acids remained unknown until recently.[16] We have shown that adducts FcP−BBr_3 (**2**) and FcP−BBr_2Fc (**3**) are readily obtained from the reaction of 3,4-dimethyl-1-phosphaferrocene (FcP) with BBr_3 and $FcBBr_2$, respectively (Fc: ferrocenyl). NMR spectroscopy using $CDCl_3$ solutions reveals a considerable amount of adduct **2** to be present in the equilibrium at ambient temperature while **3** is largely dissociated even at −50 °C (cf. theory predicts a small P−B bond-dissociation energy in **A**·BH_3 of D_e = 17.4 kcal·mol^{-1}; B3LYP/6−31G* level).[21] In the solid state, however, **1** binds not only to BBr_3, but also to $FcBBr_2$. All structural changes resulting from P−B acid−base pairing follow the same qualitative trend as those that occur in the formation of complexes of phosphaferrocene with transition metals. The experimental results obtained for **1** and **2** are also in good agreement with the theoretical calculations on **A** and **A**·BH_3. For example, the Fe−P bond is contracted by 0.085 Å upon going from **1** to **2** and by 0.050 Å upon going from **A** to **A**·BH_3. Moreover, the P(1)−B(1) bond length in **2** possesses a value of 1.972(9) Å, which is in good agreement with the theoretically predicted bond length of 1.987 Å in **A**·BH_3.[21]

The dinuclear ferrocenyl aggregate **3** contains all the key structural motifs underlying the target compound **D** (Figure 1). Work is currently in progress to synthesise corresponding coordination polymers from 1,1′-diphosphaferrocene derivatives and 1,1′-diborylferrocenes.

Experimental Section

General Remarks: All reactions and manipulations of air-sensitive compounds were carried out in dry, oxygen-free argon using standard Schlenk glassware. Solvents were freshly distilled under argon from Na/benzophenone (C_6H_6) or passed through a 4-Å molecular sieve column ($CDCl_3$) prior to use. NMR: Bruker AMX 250, AMX 400, DPX 250; abbreviations: s = singlet, d = doublet, vtr = virtual triplet, q = quadruplet, n.r. = multiplet expected in the NMR spectrum, but not resolved; n.o. = signal not observed. ^{11}B [^{31}P] NMR spectra are reported relative to external BF_3·Et_2O [H_3PO_4, 85% in water]. 3,4-Dimethylphosphaferrocene (**1**)[7,22] and dibromoborylferrocene[27] were synthesized according to literature procedures.

Syntheses

2: A solution of BBr_3 (14 mg, 0.056 mmol) in $CDCl_3$ (0.25 mL) was added in an NMR tube to a frozen solution of **1** (13 mg, 0.056 mmol) in $CDCl_3$ (0.25 mL). The reaction mixture was warmed to ambient temperature within 30 min and investigated by NMR spectroscopy. When the same quantities of BBr_3 and **1** were mixed together in toluene at −78 °C, **2** was obtained as a microcrystalline solid. Yield: 21 mg (78%). X-ray-quality crystals of **2** were grown from a highly dilute benzene solution by slow evaporation of the solvent. ^{1}H NMR (250.1 MHz, $CDCl_3$, 303 K): δ = 2.23 (s, 6 H, CH_3), 4.18 (d, $^2J_{P,H}$ = 29.1 Hz, 2 H, α-CH), 4.55 (s, 5 H, C_5H_5) ppm. ^{13}C NMR (62.9 MHz, $CDCl_3$, 303 K): δ = 15.9 (CH_3), 75.2 (C_5H_5), n.o. (C-α), n.o. (*C*CH_3) ppm. ^{11}B NMR (80.3 MHz, $CDCl_3$, 303 K): n.o. (BBr_3). ^{11}B NMR (80.3 MHz, $CDCl_3$, 223 K): δ = −20.9 (d, $^1J_{P,B}$ = 138.5 Hz, BBr_3) ppm. ^{31}P NMR (101.3 MHz, $CDCl_3$, 303 K): δ = −13.2 (n.r., $h_{1/2}$ = 30.1 Hz, phospholyl-P) ppm. ^{31}P NMR (101.3 MHz, $CDCl_3$, 223 K): δ = −12.9 (q, $^1J_{P,B}$ = 138.5 Hz, phospholyl-P) ppm.

 © 2003 Wiley-VCH Verlag GmbH & Co. KGaA, Weinheim

3: 1 (13 mg, 0.056 mmol) and $FcBBr_2$ (20 mg, 0.056 mmol) were dissolved in $CDCl_3$ (0.50 mL) at ambient temperature and the resulting mixture was sealed in an NMR tube. X-ray-quality crystals of **3** were grown from a benzene solution by slow evaporation of the solvent. Yield: 31 mg (94%). ^1H NMR (250.1 MHz, $CDCl_3$, 303 K): δ = 2.18 (s, 6 H, CH_3), 3.78 (d, $^2J_{P,H}$ = 35.5 Hz, 2 H, α-CH), 4.19, 4.23 (2 × s, 2 × 5 H, 2 × C_5H_5), 4.52, 4.91 (2 × vtr, 2 × 2 H, $^3J_{H,H}$ = $^4J_{H,H}$ = 1.8 Hz, C_5H_4) ppm. ^{13}C NMR (100.6 MHz, $CDCl_3$, 303 K): δ = 16.4 (CH_3), 71.5 (2 × C_5H_5), 78.1 (br. d, $^1J_{P,C}$ = 57.3 Hz, C-α), n.o. (*C*CH_3), 77.1, 78.2 (C_5H_4) ppm. ^{11}B NMR (80.3 MHz, $CDCl_3$, 303 K): δ = 46.1 (s, $h_{1/2}$ = 119.0 Hz, BBr_2) ppm. ^{11}B NMR (80.3 MHz, $CDCl_3$, 223 K): δ = 45.1 (s, $h_{1/2}$ = 466.2 Hz, BBr_2) ppm. ^{31}P NMR (101.3 MHz, $CDCl_3$, 303 K): δ = −81.9 (s, $h_{1/2}$ = 165.6 Hz, phospholyl-P) ppm. ^{31}P NMR (101.3 MHz, $CDCl_3$, 223 K): δ = −80.4 (s, $h_{1/2}$ = 252.8 Hz, phospholyl-P) ppm.

X-ray Crystallographic Studies

2: A single crystal (red needle; 0.06 × 0.07 × 0.31 mm) was analysed with a STOE IPDS II two-circle diffractometer with graphite-monochromated Mo-K_α radiation. An empirical absorption correction was performed using the MULABS option[28] in PLATON;[29] the minimum and maximum transmissions were 0.1676 and 0.6153, respectively. The structure was determined by direct methods using the program SHELXS[30] and refined against F^2 with full-matrix least-squares techniques using the program SHELXL-97.[31] The data/parameter ratio was 24.0. All non-hydrogen atoms were refined with anisotropic displacement parameters. Hydrogen atoms were located by difference Fourier synthesis and refined using a riding model.

3: A single crystal (orange block; 0.19 × 0.24 × 0.45 mm) was analysed with a SIEMENS SMART CCD diffractometer; repeatedly measured reflections remained stable. An empirical absorption correction using the program SADABS[32] gave a correction factor between 0.674 and 1.000. Equivalent reflections were averaged (R_{int} = 0.072). The structure was determined by direct methods using the program SHELXS.[30] Hydrogen atoms were geometrically positioned and treated as riding atoms. All non-hydrogen atoms were refined with anisotropic thermal parameters. The structure was refined on F^2 values using the program SHELXL-97.[31]

CCDC-203030 and -203031 contain the supplementary crystallographic data for this paper. These data can be obtained free of charge at www.ccdc.cam.ac.uk/conts/retrieving.html [or from the Cambridge Crystallographic Data Centre, 12 Union Road, Cambridge CB2 1EZ, UK; Fax: (internat.) + 44-1223/336-033; E-mail: deposit@ccdc.cam.ac.uk].

Acknowledgments

M. W. is grateful to the Deutsche Forschungsgemeinschaft (DFG) for financial support. M. S. wishes to thank the Fonds der Chemischen Industrie (FCI) and the Bundesministerium für Bildung und Forschung (BMBF) for a PhD grant.

[1] B. Cornils, W. A. Herrmann, *Applied Homogeneous Catalysis with Organometallic Compounds − A Comprehensive Handbook*, 2nd ed., Wiley-VCH, Weinheim, Germany, **2002**.
[2] D. W. Bruce, D. O'Hare, *Inorganic Materials*, 2nd ed., John Wiley & Sons, Chichester, UK, **1996**.
[3] A. Togni, T. Hayashi, *Ferrocenes*, Wiley-VCH, Weinheim, Germany, **1995**.
[4] I. Ojima, *Catalytic Asymmetric Synthesis*, Wiley-VCH, Weinheim, Germany **2000**.
[5] E. N. Jacobsen, A. Pfaltz, H. Yamamoto, *Comprehensive Asymmetric Catalysis*, vol. I−III, Springer, New York, USA, **1999**.
[6] P. Nguyen, P. Gómez-Elipe, I. Manners, *Chem. Rev.* **1999**, *99*, 1515−1548.
[7] F. Mathey, A. Mitschler, R. Weiss, *J. Am. Chem. Soc.* **1977**, *99*, 3537−3538.
[8] G. de Lauzon, B. Deschamps, J. Fischer, F. Mathey, A. Mitschler, *J. Am. Chem. Soc.* **1980**, *102*, 994−1000.
[9] F. Mathey, *Coord. Chem. Rev.* **1994**, *137*, 1−52.
[10] C. Ganter, L. Brassat, C. Glinsböckel, B. Ganter, *Organometallics* **1997**, *16*, 2862−2867.
[11] C. Ganter, *J. Chem. Soc., Dalton Trans.* **2001**, 3541−3548.
[12] B. Deschamps, F. Mathey, J. Fischer, J. H. Nelson, *Inorg. Chem.* **1984**, *23*, 3455−3462.
[13] M. Fontani, F. Peters, W. Scherer, W. Wachter, M. Wagner, P. Zanello, *Eur. J. Inorg. Chem.* **1998**, 1453−1465; M. Fontani, F. Peters, W. Scherer, W. Wachter, M. Wagner, P. Zanello, *Eur. J. Inorg. Chem.* **1998**, 2087.
[14] M. Grosche, E. Herdtweck, F. Peters, M. Wagner, *Organometallics* **1999**, *18*, 4669−4672.
[15] R. E. Dinnebier, M. Wagner, F. Peters, K. Shankland, W. I. F. David, *Z. Anorg. Allg. Chem.* **2000**, *626*, 1400−1405.
[16] X. Sava, M. Melaimi, N. Mézailles, L. Ricard, F. Mathey, P. Le Floch, *New. J. Chem.* **2002**, *26*, 1378−1383.
[17] K. K. Joshi, P. L. Pauson, A. R. Quazi, W. H. Stubbs, *J. Organomet. Chem.* **1964**, *1*, 471−475.
[18] G. de Lauzon, B. Deschamps, F. Mathey, *Nouv. J. Chim.* **1980**, *4*, 683−685.
[19] F. Mathey, *J. Organomet. Chem.* **1977**, *139*, 77−87.
[20] R. M. G. Roberts, J. Silver, A. S. Wells, *Inorg. Chim. Acta* **1986**, *119*, 165−169.
[21] G. Frison, F. Mathey, A. Sevin, *J. Phys. Chem. A* **2002**, *106*, 5653−5659.
[22] A. Breque, F. Mathey, P. Savignac, *Synthesis* **1981**, 983−985.
[23] S. Berger, S. Braun, H.-O. Kalinowski, *NMR-Spektroskopie von Nichtmetallen*, vol. 3 ("^{31}P- NMR-Spektroskopie"), Thieme Verlag, Stuttgart, Germany, **1993**.
[24] R. Wiest, B. Rees, A. Mitschler, F. Mathey, *Inorg. Chem.* **1981**, *20*, 2966−2970.
[25] A. Appel, F. Jäkle, T. Priermeier, R. Schmid, M. Wagner, *Organometallics* **1996**, *15*, 1188−1194.
[26] F. H. Allen, *Acta Crystallogr., Sect. B* **2002**, *58*, 380−388.
[27] T. Renk, W. Ruf, W. Siebert, *J. Organomet. Chem.* **1976**, *120*, 1−25.
[28] R. H. Blessing, *Acta Crystallogr., Sect. A* **1995**, *51*, 33−38.
[29] A. L. Spek, *Acta Crystallogr., Sect. A* **1990**, *46*, C34.
[30] G. M. Sheldrick, *Acta Crystallogr., Sect. A* **1990**, *46*, 467−473.
[31] G. M. Sheldrick, *SHELXL-97 − A Program for the Refinement of Crystal Structures*, Universität Göttingen, Göttingen, Germany, **1997**.
[32] G. M. Sheldrick, *SADABS*, Universität Göttingen, Göttingen, Germany, **2000**.

Received February 14, 2003

 © 2003 Wiley-VCH Verlag GmbH & Co. KGaA, Weinheim